# Excited-State Spectroscopy on an Individual Quantum Dot Using Atomic Force Microscopy

Lynda Cockins, Yoichi Miyahara,* Steven D. Bennett,[†] Aashish A. Clerk, and Peter Grutter

Department of Physics, McGill University, 3600 rue University, Montreal, Quebec H3A2T8, Canada

Ⓢ *Supporting Information*

**ABSTRACT:** We present a new charge sensing technique for the excited-state spectroscopy of individual quantum dots, which requires no patterned electrodes. An oscillating atomic force microscope cantilever is used as a movable charge sensor as well as gate to measure the single-electron tunneling between an individual self-assembled InAs quantum dot and back electrode. A set of cantilever dissipation versus bias voltage curves measured at different cantilever oscillation amplitudes forms a diagram analogous to the Coulomb diamond usually measured with transport measurements. The excited-state levels as well as the electron addition spectrum can be obtained from the diagram. In addition, a signature which can result from inelastic tunneling by phonon emission or a peak in the density of states of the electrode is also observed, which demonstrates the versatility of the technique.

**KEYWORDS:** *Quantum dot, Coulomb blockade, single-electron tunneling, atomic force microscopy, excited-state spectroscopy, charge sensing*
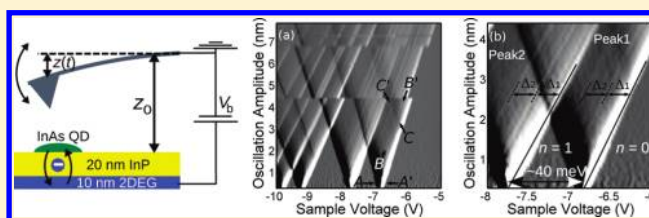
The excited state spectrum is a measure of the energy levels of a system associated with a fixed number of electrons. Experimental techniques capable of accessing this spectrum provide a useful tool for investigating quantum systems. This is especially true when the system is a quantum dot (QD), a promising potential quantum bit.[1] Here, excited states can be directly exploited for a variety of tasks. For example, when a magnetic field lifts the spin degeneracy of a discrete energy level due to the Zeeman effect, access to the excited level allows an electron to be loaded into the QD with either spin up or down orientation.[2] The excited state spectrum of a single QD can be measured optically by photoluminescence[3] or by interband optical absorption spectroscopy[4,5] with confocal microscopy, however such experiments always measure electron−hole excitations which are subject to the Coulomb interaction between electrons and holes. Although electrical transport measurements in single-electron transistor devices[6] can provide pure electronic excitation spectrum, other electrical techniques which use fewer electrodes that are spatially separated from the QD are highly valuable. They not only increase the flexibility in the types of QDs studied (since fewer strict fabrication criteria need to be met) but also reduce the invasiveness of the measurement.[7] An example is provided by charge sensing techniques, which use a highly sensitive electrometer, such as a quantum point contact[8] or single-electron transistor,[9] to probe the dot energy levels without passing an electrical current through the QD. Such techniques have recently been used to measure QD excited states: first by using a quantum point contact nearby a lateral QD[2,10] and then by using a single-electron transistor for a QD formed in a carbon nanotube.[11]

In this manuscript, we present a new and extremely versatile technique for measuring excited QD states using the dissipation of an atomic force microscope (AFM) cantilever. Previous experiments have shown that the ground state energy spectrum,[12−15] electron tunneling rate,[12,14,15] and shell structure (even without requiring a magnetic field)[16] of single dots and multidot complexes can all be measured, in addition to imaging the dot topography in situ by using an AFM cantilever as a movable charge sensor and gate. For a system consisting of a QD tunnel coupled to a charge reservoir and capacitively coupled to a conductive AFM cantilever, a bias voltage applied between the charge reservoir and cantilever tip can induce electrons to tunnel between the dot and reservoir (Figure 1).
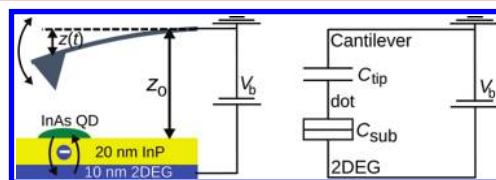
**Figure 1.** (a) Schematic of the setup. (b) Equivalent circuit diagram.

Since the AFM cantilever is acting as a scanning charge sensor as well as gate, conveniently any dot can be spatially accessed without the need for patterned electrodes anywhere on the sample. This allows for the measurement of a wide variety of
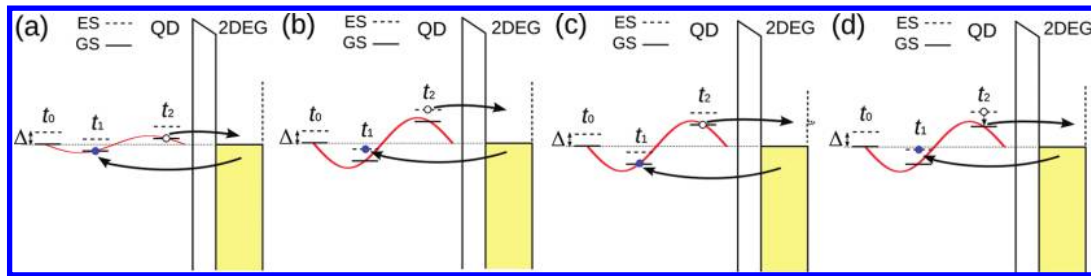
**Figure 2.** Oscillating cantilever tip (symbolized by the red curve), modulates the QD levels around. The levels are shown at three separate times, $t_0$ is the initial position of the levels, at $t_1$ and electron tunnels into the dot, and at $t_2$ an electron tunnels out of the dot. The density of states of the 2DEG are shown in yellow. The dot and 2DEG are separated by a tunnel junction. (a) A small oscillation amplitude opens an energy window that just allows tunneling into the ground state (GS). (b) The larger oscillation amplitude opens an energy window that allows tunneling into the first excited state (ES) as well as GS ($\Delta$: energy level spacing). (c) The energy window touches a region where the density of states of the 2DEG is not uniform, affecting the tunneling rate of the tunneling-out electron. (d) Inelastic tunneling process involving photon/phonon emission.
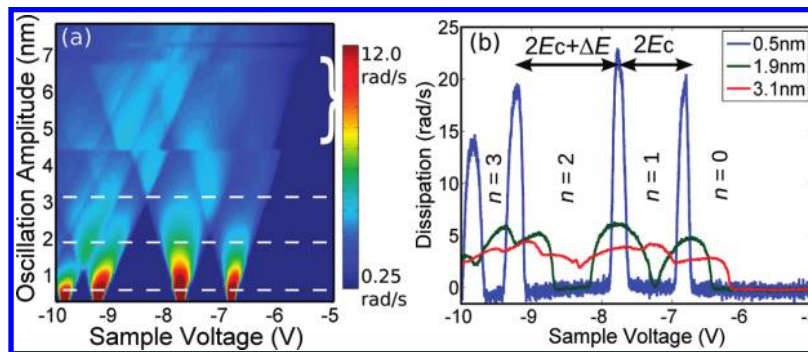


**Figure 3.** (a) Dissipation (contrast enhanced) over the dot. (b) Line profile of the dissipation at amplitudes represented with dashed lines in panel a. Each spectrum consisted of 30 000 points, taken over 30 s. The spectra in parts a and b were subjected to a 201 point moving average.

dots randomly distributed over the sample surface, such as epitaxially grown self-assembled QDs or colloidal nanoparticles, which are difficult to couple to patterned electrodes for conventional transport or charge sensing measurements. Here we provide the first measurement of the excited states of a QD by using an AFM cantilever as a charge sensor.

The experiment was performed in a home-built cryogenic AFM,[17] operated at 4.7 K. A Nanosensors PPP-NCLR cantilever, with a resonance frequency of approximately 160 kHz and nominal spring constant of 48 N/m, was used. At 4.7 K, the cantilever quality-factor was approximately 150 000. The tip-side of the cantilever was coated with a 10 nm titanium adhesion layer and a 20 nm platinum layer to ensure electrical conductivity at low temperature. A Nanosurf easyPLL was used in the self-oscillation mode for frequency detection and oscillation amplitude control. In self-oscillation mode, the cantilever is oscillated at its resonance frequency, and the oscillation amplitude of the cantilever is held constant by an automatic gain controller.[18] This allows us to simultaneously measure the shift in resonance frequency (due to conservative tip−sample interactions) and the damping (referred to as the dissipation) of the cantilever.[19] Cantilever deflection is detected by a fiber optic interferometer,[20] operating with an RF-modulated 1550 nm wavelength laser diode. As depicted in Figure 1a, the sample studied consists of uncapped InAs self-assembled QDs separated by a 20 nm InP tunneling barrier from a two-dimensional electron gas (2DEG) backelectrode formed in In$_{0.47}$Ga$_{0.53}$As quantum well.[21] The dots typically have charging energies greater than 15 meV, and so at 4.7 K we are in the Coulomb blockade regime for these dots. The charging energy of the dot is defined as $E_C = e^2/2C_\Sigma$ where $C_\Sigma =$

$C_{tip} + C_{sub}$, which is the sum of the capacitances of the tip-dot and dot-2DEG (Figure 1b).

The bias voltage $V_b$ is applied to the 2DEG layer (via an Ohmic contact formed by indium diffusion), and the cantilever is electrically grounded (Figure 1b). Tunneling between tip and dot is negligible due to the much larger tunnel barrier height of the vacuum gap as compared to the dot-2DEG barrier. Since the cantilever tip is electrostatically coupled to the dot by $C_{tip}$, the oscillating cantilever tip leads to an effective ac-gating of the electrochemical potential levels of the dot through the modulation of the lever-arm, $\alpha = C_{tip}(z(t))/[C_{tip}(z(t)) + C_{sub}]$, about a mean value which is set by $V_b$ and the mean tip-dot separation. For small oscillation amplitudes (i.e., in the weak coupling regime[16]), when $V_b$ is tuned to a point of QD charge degeneracy, single-electron tunneling from the 2DEG is possible, causing the dot to fluctuate between its $n$ and $n + 1$ electron ground states. Although $n$ stochastically fluctuates due to the tunneling, its average value follows the oscillating tip motion, subjecting the cantilever tip to an oscillating electrostatic force.[16] The finite average time between tunnel events causes a 90° out-of-phase as well as in-phase component of the oscillating force with respect to the cantilever motion. These two components lead to increased cantilever dissipation and a shift in the cantilever resonance frequency, respectively.[12,14,15] Increasing the cantilever oscillation amplitude will eventually modulate the energy levels of the dot so much that an electron can tunnel between $n$ electron ground state and $n + 1$ electron excited states. This is demonstrated by the schematic in Figure 2. The new tunneling processes involving excited states also contribute to the dot-induced cantilever dissipation, causing it to increase.[16] By taking the derivative of the dissipation with respect to $V_b$ we can detect these small changes, and thereby

measure the energy separations of the excited states ($\Delta_1$, $\Delta_2$, etc.).

In order to measure the excited states, the cantilever tip was placed over the center of an isolated dot (see the Supporting Information, Figure S1) with a mean tip–sample separation of 20 nm and the $V_b$ was swept for different oscillation amplitudes while the distance-regulating feedback was shut off. Figure 3a consists of 67 dissipation versus $V_b$ spectra taken with different cantilever oscillation amplitudes and the three representative spectra are shown in Figure 3b. Such a spectrum taken at small amplitude resembles Coulomb oscillation peaks observed in transport spectroscopy and is indeed an electron addition spectrum (i.e., it measures the transition between $n$-electron and $(n + 1)$-electron ground states). The shift marked by the white curly bracket in Figure 3a is caused by a charge rearrangement somewhere near the dot.

As clearly observed in Figure 3b, the height of the dissipation peaks decreases with increasing cantilever oscillation amplitude. The decrease and broadening of the peaks result from the change of the probability distribution of the position of the oscillating cantilever tip: the cantilever is spending less of its cycle near the position that leads to maximal tunneling, but it is hitting this condition over a larger range of voltages. As described in ref 16, the highly asymmetric peak shape (most noticeable for the 1.9 nm oscillation amplitude spectrum in Figure 3b) occurs because of degenerate energy levels within the dot: the first half of the peaks within a set of degenerate levels will always be skewed in the same direction along the energy axis, while the latter half will be skewed in the opposite direction. Figure 3a,b clearly shows that the first two peaks are skewed away from each other, meaning that these peaks belong to a single spin-degenerate orbital level. Although the third peak is clearly skewed to the right, the directionality of the fourth peak is difficult to discern. Included in the Supporting Information is a single-electron addition spectrum (Figure S2) which clearly shows that the fourth peak is skewed in the opposite direction to the third peak, to the left, and therefore these two peaks belong to another spin-degenerate orbital level which is not degenerate with the next orbital level.

Figure 4 shows the dissipation derivative with respect to $V_b$, with a zoom on the first two rightmost peaks. The derivative of the broadened dissipation peaks look like down-pointing triangles. As one increases the magnitude of $V_b$ (i.e., moves right to left), the rightmost bright white line of each triangle corresponds to the transition from Coulomb blockade to where the number of electrons on the dot can fluctuate between $n$ and $n + 1$ by single-electron tunneling, and the dark line corresponds to the transition from this fluctuating region to the Coulomb blockade state with $n + 1$ electrons on the dot. The feature shown in $A$–$A'$ in Figure 4a results from the single-electron tunneling between the ground state level of the QD and 2DEG and the process is depicted in Figure 2a.

The main features of interest in Figure 4 are the lines that run parallel to the rightmost triangle edges (e.g., $B$–$B'$). The parallel lines result from the opening of additional tunneling paths once excited states become accessible within the energy window set by the top and bottom swing of the cantilever oscillation (Figure 2b). In Figure 4b, showing only the first (right) and second (left) peaks, two lines are visible on the first peak (the first marked $B$–$B'$) and two are visible on the second. At larger oscillation amplitudes, more lines corresponding to the higher excited states are resolved as can be seen in Figure 4a. While these features are consistent with excited state
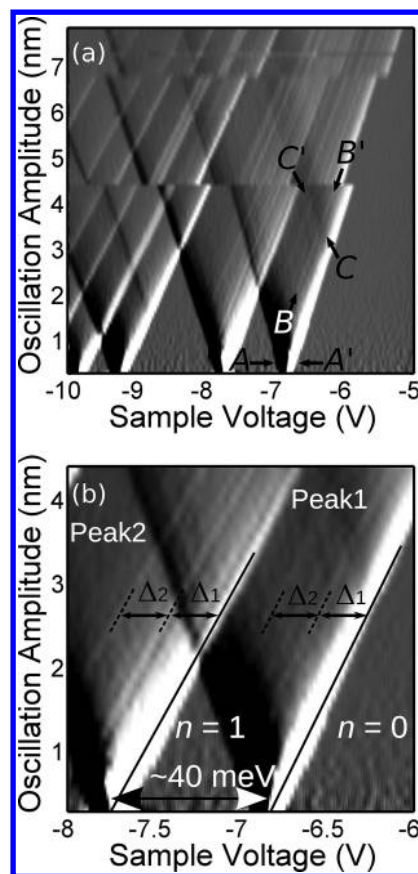


**Figure 4.** (a) Derivative of dissipation data in Figure 3a (subjected to a 151 point moving average). (b) Close up of the first (right) and second (left) peaks in (a). Lines are overlaid to guide the eyes.

tunneling, they could also be due to other, more extrinsic, effects (e.g., photon/phonon assisted inelastic tunneling and features in the density of states of the reservoir). While all these effects are of great interest, the unambiguous identification of their roles in our system requires more detailed study, as discussed extensively in a recent review.[22] We, however, stress that our main result is to show that the present technique is capable of resolving such features, regardless of their origin.

Here we discuss a possible scenario based on the assumption that the observed features ($B$–$B'$) originate from the orbital excited states of the dot. Using the measured lever arm ($\alpha = 0.042 \pm 0.003$: the detail found in Supporting Information), the dissipation spectrum acquired with the smallest oscillation amplitude directly provides an energy spacing between the first two Coulomb blockade peaks $E_{add}^{n=2} = 2E_C^{n=2} = 40$ meV, and between the second and third peaks, $E_{add}^{n=3} = 2E_C^{n=3} + \Delta E = 62$ meV (Figure 3b). Here, $\Delta E$ is the orbital level spacing obtained from the addition spectra, and we have allowed for the effective charging energy $E_C$ (i.e., the interaction contribution to the addition energy) to be $n$ dependent. In the commonly used constant interaction model (CI),[23] $E_C$ is independent of $n$ (i.e., $E_C^{n=2} = E_C^{n=3}$), and thus our addition-spectrum measurement would directly yield $\Delta E = 22$ meV. This value for the level spacing obtained from the addition spectrum is inconsistent with what we measure from the excited-state spectra (via the large-oscillation cantilever dissipation spectra, Figure 4). From these spectra, we found the level spacings of the first two orbital excited states are: $\Delta_1 = \Delta_2 = 11$ meV for $n = 1$ and $\Delta_1 = \Delta_2 = 12$ meV for $n = 2$.

The above discrepancy between the level spacing extracted from the addition spectrum ($\Delta E$) and from the large-oscillation dissipation ($\Delta_1$) could result from two different causes. First, adding a single electron to the dot could change the dot confinement potential and hence the level spacing; similar effects have been seen in other QD systems.[23,24] Second, interaction effects beyond the CI model could be significant. A Hartree−Fock treatment[25] of a few-electron QD shows that the effective charging energy for adding the third electron $[E_C^{n=3}]$ should be less than that for adding the second $[E_C^{n=2}]$; this is the result of exchange interactions, as well as the difference between interorbital and intraorbital direct interactions. In contrast, if we assume $\Delta E = \Delta_1$, our addition energies are consistent with $E_C^{n=3} > E_C^{n=2}$. Although this could be explained by a large antiferromagnetic exchange interaction, such an interaction is inconsistent with microscopic calculations.[25] We thus believe that the first mechanism mentioned above is the more plausible explanation. In either of the above scenarios, the advantage of being able to directly measure the excited state spectrum at fixed $n$ is clear: it provides a direct method for measuring the level spectrum, without needing to make any assumption about whether $E_C$ or the dot potential are dependent on the number of dot electrons. We note that excited-state spectroscopy of an ensemble of self-assembled InAs QDs grown on a GaAs substrate has previously been reported. This was done by combining capacitance spectroscopy and far-infrared transmission spectroscopy which probes intraband absorption.[26,27] Reference 27 obtained the $n$-dependent charging energy and observed $E_C^{n=3} < E_C^{n=2}$. This apparent discrepancy might point to the different electronic structure of uncapped versus capped QDs, a topic which deserves more detailed investigation. We stress that, unlike the technique of ref 27, our approach allows one to directly probe the excitation of a single QD without optical measurement.

Another feature of interest is the resonant line marked $C-C'$ in Figure 4a which occurs ∼40−50 meV from the $n = 1$ ground state; it cannot be explained by the tunneling electron accessing higher energy levels of the dot. The slope of $C-C'$ indicates that the mechanism involves a tunneling-out process.[22] We however confirmed that the dot is empty prior to the first peak as no more peaks are observed in the frequency shift or dissipation for $-6\,V< V_b <+ 5\,V$, meaning that $C\text{-}C'$ cannot be caused by an electron tunneling out of lower lying energy levels of the dot. Possible causes of $C-C'$ are thus a peak in the density of states of the 2DEG, or an inelastic tunneling pathway. A peak in the density of states of the 2DEG affects the electron tunneling rate, and can lead to abrupt changes in the dissipation which are enhanced in the dissipation derivative. This commonly observed feature,[6,28] which provides an avenue for probing the density of states of the reservoir itself,[22] is depicted in Figure 2c.

Alternatively the $C-C'$ feature may be caused by a new tunneling pathway where inelastic tunneling is enabled by the emission of a phonon (the slope of $C-C'$ is indicative of emission). The process is depicted in Figure 2d. The energy of $C-C'$ (40−50 meV) is similar to that of the longitudinal optical (LO) phonon modes of InAs QDs grown on InP measured by Raman spectroscopy.[29] Here, the phonon energy corresponds most closely to the LO phonon in the InP tunneling barrier as reported by ref 29, with the other possibilities being the InAs dot, the 2DEG, or one of the interfaces between them. We remark that the origin of $C-C'$ could be resolved by measuring $C-C'$ as a function of magnetic field: if caused by phonon

emission, it will not change as a function of magnetic field, while if due to the density of states of the 2DEG then a Zeeman splitting of $C-C'$ would occur which reflected the $g$-factor of the 2DEG.[22] The capability of detecting inelastic tunneling processes offers the prospect of inelastic tunneling spectroscopy[30] in nano/atomic scale tunnel junctions.

In conclusion, we have demonstrated that an AFM can be used to not only measure the addition energy spectrum but also the excited states of a quantum dot. In addition an interesting feature was observed, resulting from a change in electron tunneling rate, which could be attributed to the detection of a phonon mode or change in the density of states of the reservoir. The high spatial resolution of the AFM in combination with the ability to measure the energy levels of confined electronic systems allows for the ability to study systems which are difficult to contact with electrodes. Potential examples of other such systems would be impurity or donor atoms, or molecules on insulating surfaces.

## ■ ASSOCIATED CONTENT

### Ⓢ Supporting Information

Atomic force microscope images of quantum dot; determining the dot level degeneracies from the dissipation peaks asymmetry; and dissipation spectrum over quantum dot at 28 K: determining the tunneling rate and lever arm. This material is available free of charge via the Internet at http://pubs.acs.org.

## ■ AUTHOR INFORMATION

### Corresponding Author
*E-mail: yoichi.miyahara@mcgill.ca.

### Present Address
†Department of Physics, Harvard University, 17 Oxford Street, Cambridge, Massachusetts 02138, United States.

## ■ REFERENCES

(1) Loss, D.; DiVincenzo, D. P. *Phys. Rev. A* **1998**, *57*, 120.
(2) Elzerman, J. M.; Hanson, R.; Beveren, L. H. W. v.; Vandersypen, L. M. K.; Kouwenhoven, L. P. *Appl. Phys. Lett.* **2004**, *84*, 4617−4619.
(3) Warburton, R.; Schaflein, C.; Haft, D.; Bickel, F.; Lorke, A.; Karrai, K.; Garcia, J.; Schoenfeld, W.; Petroff, P. *Nature* **2000**, *405*, 926−9.
(4) Urbaszek, B.; Warburton, R.; Karrai, K.; Gerardot, B.; Petroff, P.; Garcia, J. *Phys. Rev. Lett.* **2003**, *90*, 247403.
(5) Högele, A.; Seidl, S.; Kroner, M.; Karrai, K.; Warburton, R.; Gerardot, B.; Petroff, P. *Phys. Rev. Lett.* **2004**, *93*, 217401.
(6) Kouwenhoven, L. P.; Oosterkamp, T. H.; Danoesastro, M. W. S.; Eto, M.; Austing, D. G.; Honda, T.; Tarucha, S. *Science* **1997**, *278*, 1788−1792.
(7) Hanson, R.; Kouwenhoven, L. P.; Petta, J. R.; Tarucha, S.; Vandersypen, L. M. K. *Rev. Mod. Phys.* **2007**, *79*, 1217.
(8) Field, M.; Smith, C. G.; Pepper, M.; Ritchie, D. A.; Frost, J. E.; Jones, G. A.; Hasko, D. G. *Phys. Rev. Lett.* **1993**, *70*, 1311−1314.
(9) Lafarge, P.; Pothier, H.; Williams, E. R.; Esteve, D.; Urbina, C.; Devoret, M. H. *Z. Phys. B: Condens. Matter* **1991**, *85*, 327−332.

(10) Otsuka, T.; Abe, E.; Iye, Y.; Katsumoto, S. *Appl. Phys. Lett.* **2008**, *93*, 112111.

(11) Gotz, G.; Steele, G. A.; Vos, W.-J.; Kouwenhoven, L. P. *Nano Lett.* **2008**, *8*, 4039−4042.

(12) Woodside, M. T.; McEuen, P. L. *Science* **2002**, *296*, 1098.

(13) Zhu, J.; Brink, M.; McEuen, P. L. *Appl. Phys. Lett.* **2005**, *87*, 242102.

(14) Zhu, J.; Brink, M.; McEuen, P. L. *Nano Lett.* **2008**, *8*, 2399−2404.

(15) Cockins, L.; Miyahara, Y.; Bennett, S. D.; Clerk, A. A.; Studenikin, S.; Poole, P.; Sachrajda, A.; Grutter, P. *Proc. Natl. Acad. Sci. U.S.A.* **2010**, *107*, 9496−9501.

(16) Bennett, S. D.; Cockins, L.; Miyahara, Y.; Grutter, P.; Clerk, A. A. *Phys. Rev. Lett.* **2010**, *104*, 017203−017207.

(17) Roseman, M.; Grutter, P. *Rev. Sci. Instrum.* **2000**, *71*, 3782.

(18) Albrecht, T. R.; Grütter, P.; Horne, D.; Rugar, D. *J. Appl. Phys.* **1991**, *69*, 668−673.

(19) Durig, U.; Steinauer, H. R.; Leblanc, N. *J. Appl. Phys.* **1997**, *82*, 3641.

(20) Rugar, D.; Mamin, H. J.; Guethner, P. *Appl. Phys. Lett.* **1989**, *55*, 2588.

(21) Poole, P. J.; McCaffrey, J.; Williams, R. L.; Lefebvre, J.; Chitrani, D. *J. Vac. Sci. Technol.* **2001**, *B19*, 1467.

(22) Escott, C. C.; Zwanenburg, F. A.; Morello, A. *Nanotechnology* **2010**, *21*, 274018.

(23) Sohn, L. L.; Kouwenhoven, L. P.; Schon, G., Eds.; *Mesoscopic Electron Transport*; Kluwer Academic: Dordrecht, The Netherlands, 1997.

(24) Postma, H. W. C.; Yao, Z.; Dekker, C. *J. Low Temp. Phys.* **2000**, *118*, 495.

(25) He, L.; Zunger, A. *Phys. Rev. B* **2006**, *73*, 115324.

(26) Drexler, H.; Leonard, D.; Hansen, W.; Kotthaus, J. P.; Petroff, P. M. *Phys. Rev. Lett.* **1994**, *73*, 2252.

(27) Fricke, M.; Lorke, A.; Kotthaus, J. P.; Medeiros-Ribeiro, G.; Petroff, P. M. *Europhys. Lett.* **1996**, *36*, 197−202.

(28) Möttönen, M.; Tan, K. Y.; Chan, K. W.; Zwanenburg, F. A.; Lim, W. H.; Escott, C. C.; Pirkkalainen, J.-M.; Morello, A.; Yang, C.; van Donkelaar, J. A.; Alves, A. D. C.; Jamieson, D. N.; Hollenberg, L. C. L.; Dzurak, A. S. *Phys. Rev. B* **2010**, *81*, 161304.

(29) Groenen, J.; Priester, C.; Carles, R. *Phys. Rev. B* **1999**, *60*, 16013−16017.

(30) Galperin, M.; Ratner, M. A.; Nitzan, A. *J. Phys.: Condens. Matter* **2007**, *19*, 103201.